IVYSPRING INTERNATIONAL PUBLISHER

Theranostics

2012; 2(12):1199-1207. doi: 10.7150/thno.4812

Research Paper

Dual-Modality, Dual-Functional Nanoprobes for Cellular and Molecular Imaging

Jyothi U. Menon[1], Praveen K. Gulaka[2], Madalyn A. McKay[1], Sairam Geethanath[2], Li Liu[1] and Vikram D. Kodibagkar[1,2,3,✉]

1. Department of Radiology, UT Southwestern Medical Center at Dallas, Dallas, TX, USA;
2. Joint program in Biomedical engineering at UT Arlington and UT Southwestern Medical Center at Dallas, Dallas, TX, USA;
3. School of Biological and Health Systems Engineering, Arizona State University, Tempe, AZ, USA.

✉ Corresponding author: Vikram D. Kodibagkar, Ph D. School of Biological and Health Systems Engineering, Arizona State University Tempe, AZ, 85287-9709 Email: Vikram.Kodibagkar@asu.edu.

Received: 2012.07.03; Accepted: 2012.12.29; Published: 2012.12.31

Abstract

An emerging need for evaluation of promising cellular therapies is a non-invasive method to image the movement and health of cells following transplantation. However, the use of a single modality to serve this purpose may not be advantageous as it may convey inaccurate or insufficient information. Multi-modal imaging strategies are becoming more popular for *in vivo* cellular and molecular imaging because of their improved sensitivity, higher resolution and structural/functional visualization. This study aims at formulating Nile Red doped hexamethyldisiloxane (HMDSO) nanoemulsions as dual modality (Magnetic Resonance Imaging/Fluorescence), dual-functional (oximetry/detection) nanoprobes for cellular and molecular imaging. HMDSO nanoprobes were prepared using a HS15-lecithin combination as surfactant and showed an average radius of 71±39 nm by dynamic light scattering and *in vitro* particle stability in human plasma over 24 hrs. They were found to readily localize in the cytosol of MCF7-GFP cells within 18 minutes of incubation. As proof of principle, these nanoprobes were successfully used for fluorescence imaging and for measuring pO_2 changes in cells by magnetic resonance imaging, *in vitro*, thus showing potential for *in vivo* applications.

Key words: hexamethyldisiloxane; Nile Red; nanoemulsions; MR oximetry; fluorescence; dual-modality.

Introduction

Hypoxia is a condition often found in solid tumors, where insufficient oxygen is available for cells to carry out their metabolic activities. As a result, these cells switch from aerobic mode of metabolism to the anaerobic glycolysis pathway in order to proliferate [1]. In addition to promoting tumor angiogenesis and metastasis, hypoxia can also make tumors resistant to radiation therapy and chemotherapy by reducing the bioavailability of molecular oxygen which acts as a radiosensitizer [2, 3]. The occurrence of hypoxia, however, is not restricted to tumor regions alone. It also plays a key role in determining the survival and growth of tissue engineered scaffolds *in vivo*. Cells within an engineered construct experiences hypoxia initially on implantation, until new blood vessels are recruited to the area [4]. According to previous reports, an oxygen gradient can be observed within three-dimensional bone constructs due to high cell proliferation. This can result in hypoxia particularly in the central regions of the scaffold, causing cell death [5]. Hypoxia and absence of nutrients can also cause massive mesenchymal cell death which renders the construct seeded with them, unviable [6]. It is therefore necessary to monitor oxygen levels within

tissue engineered constructs to determine their fate after implantation. Additionally, studies on mouse embryonic stem cells have shown oxygen-dependent differentiation and proliferation into neural cells *in vitro* [7]. A method of monitoring hypoxic conditions would thus be important to prognosticate stem cell growth and viability both *in vitro* as well as *in vivo* following implantation.

The past two decades have seen an increased interest in developing MR contrast agents for cellular and molecular imaging. Gadolinium chelates, superparamagnetic iron oxide (SPIO) particles and have all been used as imaging agents to non-invasively monitor cellular processes or the behavior of macromolecules in vivo [8]. Earlier, MRI methods were widely used for visualization and tracking of implanted cells, based on the contrast generated by the internalization of iron oxide particles [9-11]. More recently, perfluorocarbon (PFC) emulsions have been successfully used for cell labeling and tracking [12-16]. PFC nanoemulsions have also been used in ^{19}F MR oximetry based on the sensitivity of the perfluorocarbon fluorine resonance spin lattice relation time (T_1) to pO_2. Several fluorescence as well as magnetic resonance (MR) techniques are currently in use to measure oxygenation in tissues [17, 18]. As an alternative approach, our lab recently demonstrated that hexamethyldisiloxane (HMDSO) could be used to quantitatively measure oxygen tension (pO_2) in tissues using ^1H MR [19, 20] and we have developed HMDSO-based nanoemulsions as pO_2 nanoprobes [21] . Submicron and nanoemulsions have been established and used as drug delivery systems for solubilization of poorly water-soluble drugs and imaging probes, reduction in toxicity and, targeted delivery to various organs [22]. The current study demonstrates the formulation and application of Nile Red-doped, HMDSO-loaded, nanoemulsions as nanoprobes for dual modality (MRI/fluorescence) dual functional (detection/oximetry) cellular and molecular imaging. Fluorescence imaging offers sensitive detection of fluorochromes at nanomolar concentrations and allows simultaneous multispectral imaging of several biological processes. These attributes are complementary to those of MRI such as high spatial resolution, excellent soft tissue contrast, and ability to image tissue function and makes the combination of MRI with fluorescence imaging highly desirable. Correspondingly, there has been much interest recently in development of dual-modality MRI-fluorescence probes[23-31]. For targeting and cell-labeling applications [32-35] (e.g. stem cells) dual modality probes offer additional advantage of enabling ex-vivo validation by fluorescence microscopy.

Materials and methods

General

HMDSO and Nile Red dye were purchased from Sigma Aldrich (St Louis, MO, USA) while Soybean Lecithin was purchased from MP Biomedicals, LL (Solon, OH) respectively. Solutol HS15 was a gift from BASF Corporation (Ludwigshafen, Germany). MCF7-wild type breast cancer cells (ATCC) were stably transfected with green fluorescent protein (GFP) gene in our lab. NIH-3T3 fibroblast cells were kindly provided by Prof. Liping Tang of University of Texas at Arlington.

Formulation and characterization of nanoprobes

The dual-modality nanoprobes were prepared by modifying the procedure used by us previously [21] to synthesize MRI based pO_2 nanoprobes. The modification involved addition of a second surfactant, soybean lecithin, for improved stability [36]. Briefly, a 2% v/v HS15: 1% w/v soybean lecithin surfactant mixture, in de-ionized water, was used to emulsify a payload of Nile Red (0.25 mM) dye in HMDSO. Surfactant was heated to ~60^{o}C while stirring for 2 minutes. Once the surfactant solution became slightly translucent, HMDSO/Nile Red mixture was added drop-wise so that the final emulsion would have 40% (v/v) HMDSO and 0.1 mM Nile Red dye and continued to be stirred while heating for 15 minutes. This starting emulsion was then subject to high power probe ultrasonication and extrusion filtration [21], to obtain the dual modality nanoprobes.

Particle size measurements were carried out using DynaPro Titan dynamic light scattering (DLS) instrument (Wyatt Technology Corporation, Santa Barbara, CA, USA). The results from the DLS were correlated with observation of the nanoprobes using TEM (FEI Tecnai G2 Spirit BioTWIN, Hillsboro, OR) negatively stained with phosphotungstic acid. Finally, the presence of HMDSO in the nanoprobes after synthesis was confirmed using Varian INOVA 400 MHz NMR.

In vitro stability and cytotoxicity studies

At pre-determined time points (0, 1, 2, 5 and 24 hours) post synthesis in de-ionized water, the particle size was measured using DLS to check for aggregation and/or variation in particle sizes(n=5 replicates). To study the stability in human plasma, the nanoprobes were added to a 50% plasma solution and maintained at 37^{0}C and particle size was measured over time, as above.

To assess cytotoxicity, 3T3 fibroblast cells were

seeded in a 48 well plate at a density of 10^5 cells per well and incubated for 24 hours to allow the cells to attach to the bottom of the wells. These cells were then incubated with the nanoprobes at increasing concentrations for 4 hours. The experiment was conducted in triplicates for each concentration. At the end of the 4-hour incubation, the media was removed and the cells were washed with PBS. The PBS was then replaced with fresh media and the appropriate ratio of MTS assay solution (Promega Corporation, Madison, WI, USA) per well. Following 1 hour incubation with MTS assay, cell viability was measured using a microplate reader at an absorbance wavelength of 490 nm. The same procedure was repeated using varying concentrations of the surfactant combination.

Live cell imaging of nanoprobe uptake

To study the uptake and localization of the nanoprobes, MCF7-GFP cells were first seeded at a density of 90,000 cells per well in a glass bottom dish and incubated for 2 days prior to the experiment. The dishes were placed in a 5% CO_2 environment within the confocal microscope (Zeiss LSM 50) chamber for 30 minutes to allow the cells to settle down. Based on the results of the cytotoxicity study, nanoprobes were added to the cells at the beginning of the experiment to a concentration of 0.2% v/v in media. The MCF7-GFP cells were imaged for 30 minutes at 2-minute intervals using excitation wavelengths of 488 nm and 561 nm for GFP and Nile Red, respectively. The images were processed from z-scans of 1µm thickness using ImageJ software.

Dual modality studies on Matrigel™ phantoms

MRI and Fluorescence imaging were carried out to test the utility of the synthesized nanoprobes for dual modality/ dual functional application of the nanoprobes. To prepare the sample, 100 µl of phenol red-free BD Matrigel™ basement membrane matrix containing 5 x 10^6 wild type MCF7 cells, devoid of media, were added to a 2 mL tube. The cell-matrigel mixture was allowed to gel at room temperature for about 2 minutes. Then, 200 µl of the matrigel was added to the tube to form a separate layer above the matrigel layer containing cells and allowed to gel. Matrigel-nanoprobe mixture (700 µl, 10:1) was added and allowed to set at room temperature. The tubes were immediately sealed to prevent further entry of oxygen into the tubes. Fluorescence imaging was performed using CRi Maestro imaging system. MRI studies were performed on a Varian 4.7T MRI scanner (Agilent Inc., Palo Alto, CA, USA). Following acquisition of water and HMDSO resonance selective spin-echo MR images, oximetry was performed over 4 hrs using the PISTOL technique [19] to measure changes in partial pressure of oxygen due to oxygen consumption using a previously published calibration curve [21] that relates the relaxation times measured by PISTOL to quantitative pO_2 values. Voxel-wise statistical comparisons (one way ANOVA) were made using MATLAB on the pO_2 values.

RESULTS

Formulation and characterization of nanoprobes

The size of the nanoemulsion formulations was obtained using DLS and compared with semi-automated image analysis from the TEM image (Figure 1). The use of phosphotungstic acid enabled the visualization of nanoprobes by a negative contrast effect (light on a dark, electron-dense background). The average radius as measured by DLS was 71±39 nm while that from TEM was 58±33 nm. The spectra obtained using ^{1}H NMR showed a distinct HMDSO peak at around 0.02 ppm, well separated from the water peak at 4.7 ppm. The ratio between the HMDSO and water peak areas from the NMR spectrum was observed to be 0.69. To determine the stability of the nanoprobes in DI water and 50% human plasma, radii were measured by DLS at fixed time-points for up to 24 hours. The nanoprobes showed good stability in both de-ionized water as well as plasma for the entire duration of the experiment (Figure 2) and showed no significant aggregation between the probes. Studies were also conducted to analyze in vitro biocompatibility of nanoprobes and the surfactant combination using NIH 3T3 fibroblast cells. While 3T3 cells maintained close to 100% viability at all concentrations of the surfactant combination tested, they achieved IC_{50} at a nanoprobe concentration at around 0.4% (v/v) (Figure 3).

In vitro cellular uptake of nanoprobes

To study time-dependent uptake of the nanoprobes, MCF7-GFP cells were incubated with nanoprobes and imaged for half an hour at 2-minute intervals (Figure 4 A). Confocal microscopy showed the localization of the nanoprobes within the cytosol. Measurement of mean intensities in a region of interest within a cell showed that the GFP fluorescence remained constant throughout the duration of the experiment while Nile Red fluorescence increased substantially over time (Figure 4B). A gradual but distinct increase in Nile red fluorescence could be observed within the cytosol of MCF7-GFP cells for the first 18 minutes of incubation followed by a more rapid uptake subsequently. The Nile red fluorescence

intensity was not observed to saturate till the end of the observation period (30 min) indicating that further uptake of nanoprobes was possible beyond 30 min.

Dual modality studies on Matrigel™ phantoms

MR and Fluorescence imaging was carried out on tightly-sealed samples containing both the nanopobes as well as MCF7 cells to study the dual functionality of the nanopobes (Figure 5A). Fluorescence could be easily detected in the layer containing the nanoprobes indicating that they could be potentially detected using fluorescence imaging *in vivo* at these concentrations. PISTOL imaging showed a gradual decrease in pO_2 within the sample for 4 hours as the cells metabolized the existing oxygen within the tube (Figure 5B). A one-way ANOVA comparing pO_2 values (n=36 voxels) over 8 time-points (spanning 4 hrs) showed that the decrease in pO_2 was statistically significant ($p<<0.001$). A clear oxygen gradient was observed with the region closer to the cell layer showing higher oxygen depletion over time with pO_2 values~ 40 torr. Fitting the mean pO_2 value using an exponential decay curve $pO_2(t)= A+B*e^{-kt}$ yielded fit constants A= 83 ±5 torr, B=78 ±5 torr and k= (6.1± 0.8)X10^{-3} min^{-1} (R^2 =0.996). Based on these pO_2 kinetic parameters and assuming an oxygen solubility of 7.6 mg/mL, the initial oxygen consumption rate can be calculated to be 0.10 nmole/10^6 cells/min which reduces to 0.03 nmole/10^6 cells/min at 4 hrs.

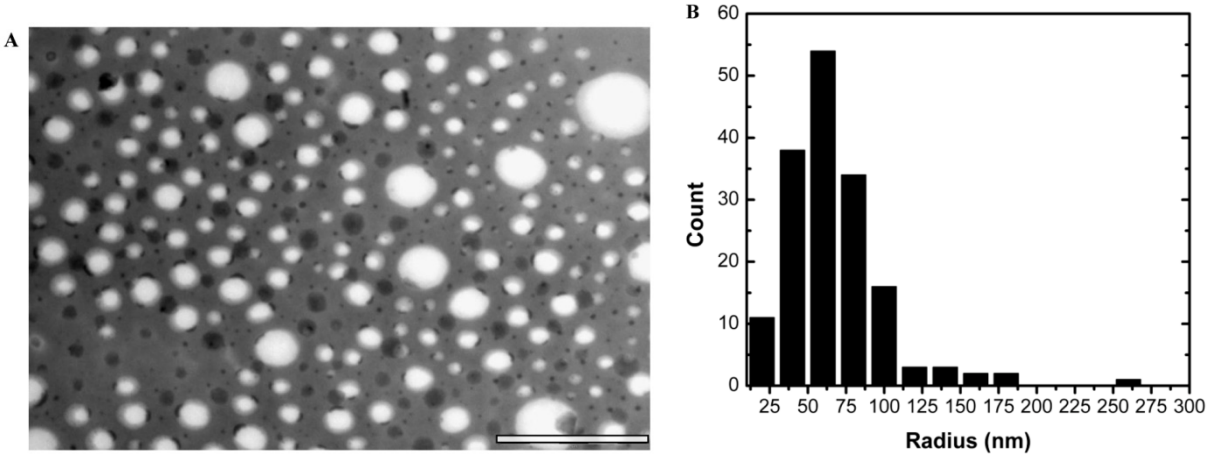

Figure 1: Particle characterization: **(a)** TEM images of the nanoprobes stained negatively with 0.5% phosphotungstic acid and **(b)** corresponding size analysis using ImageJ. (scale bar =1 um)

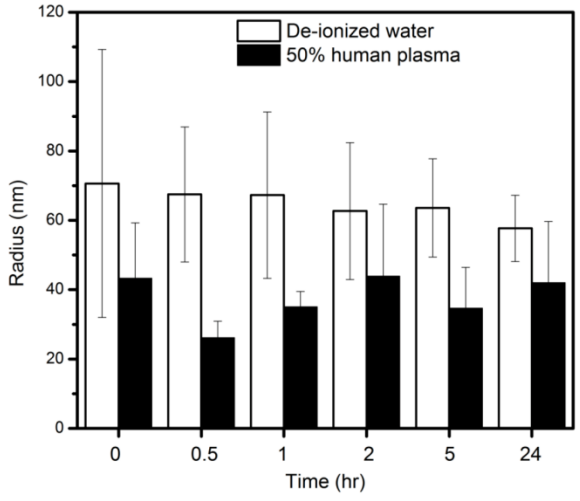

Figure 2: Particle stability study: Particle size of nanoprobes in deionized (DI) water and 50% human plasma measured by dynamic light scattering (DLS) over 24 hr.

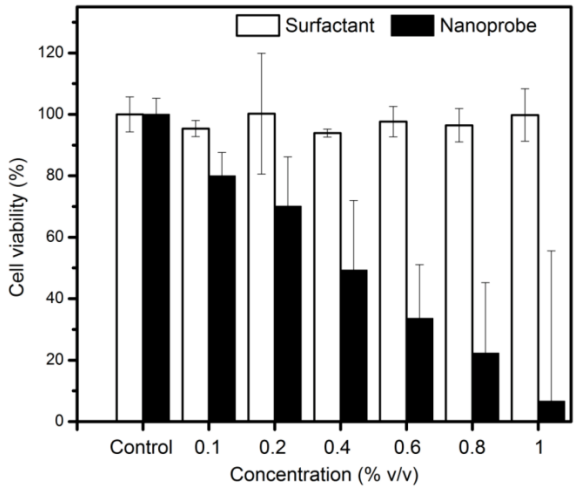

Figure 3: Cytotoxicity assay: 3T3 fibroblast viability assessed at different concentrations of surfactants and nanoprobes.

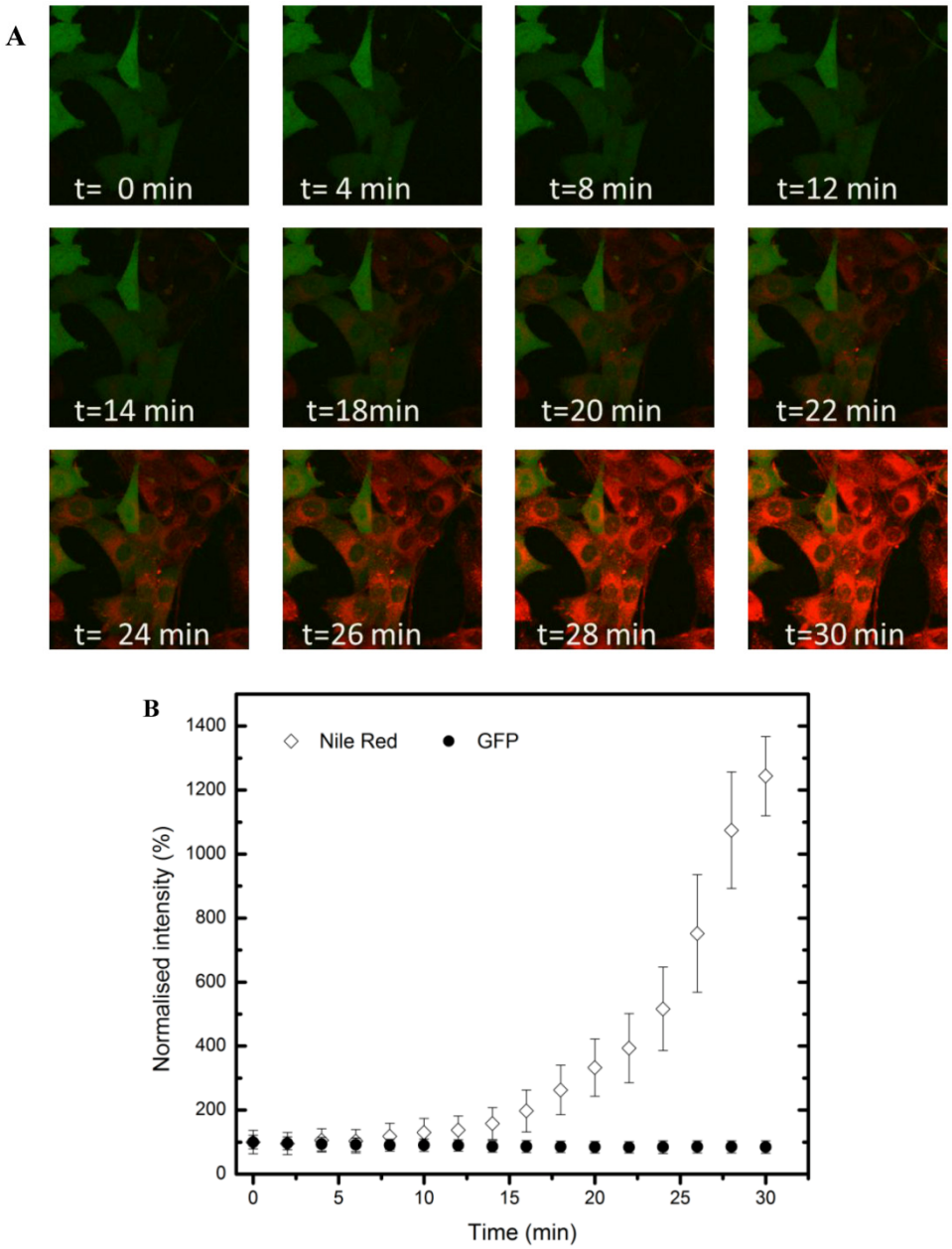

Figure 4: Live cell imaging: **(A)** Confocal microscopy composite images showing time-dependent uptake of the nanoprobes by MCF7-GFP cells over a period of 30 mins. **(B)** Graphical representation of changes in Nile red and GFP fluorescence over time within a region of interest in a MCF7-GFP cell cytoplasm.

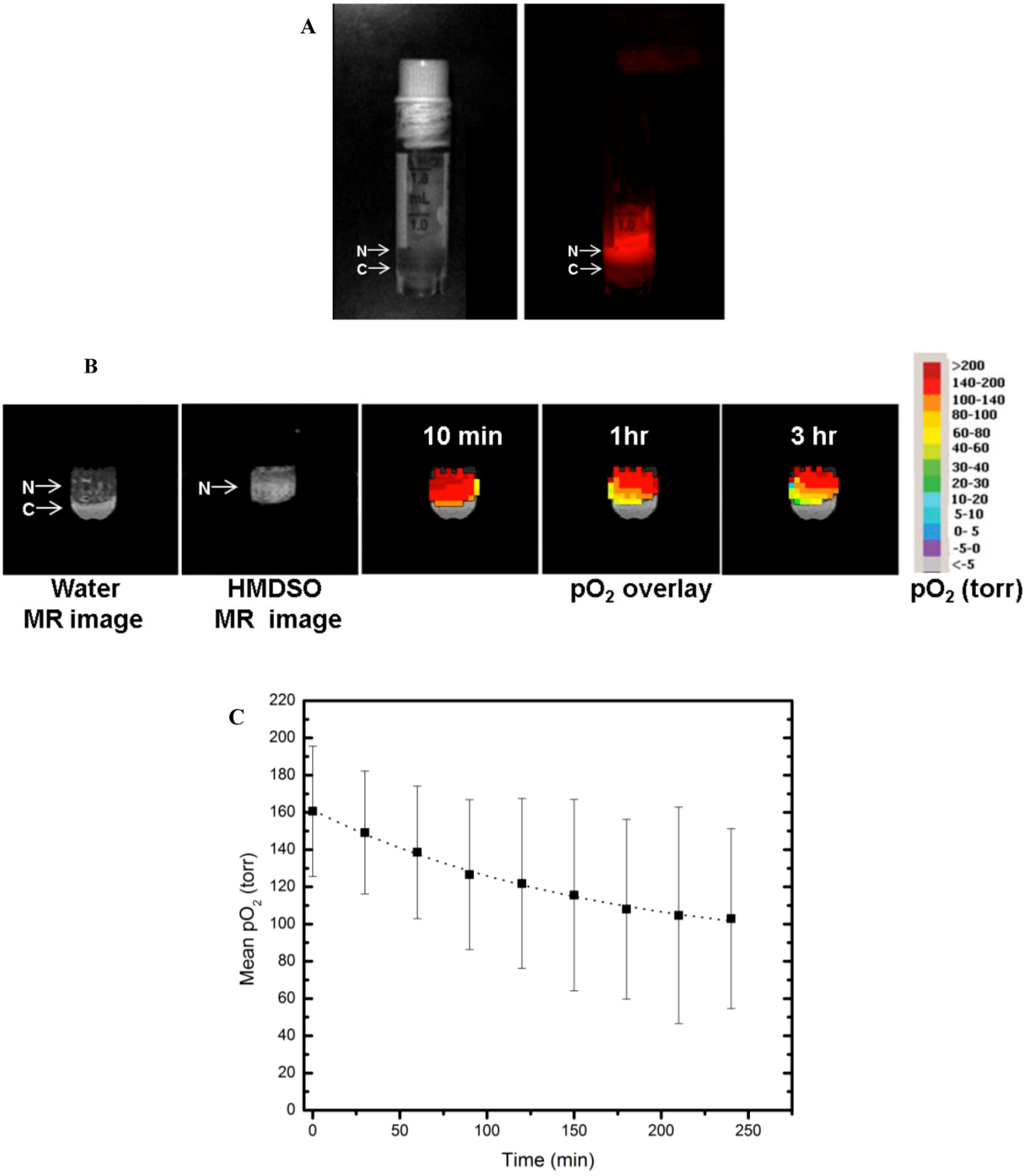

Figure 5: Dual modality (MR and Fluorescence) imaging: **(A)** White light (left) and fluorescence (right) images of sample containing the nanoprobes (N) and 5 X10^6 MCF7 cells (C) in separate layers. **(B)** MR imaging of the same sample allows visualization of the nanoprobes and oximetry using the PISTOL technique as well as pO_2 changes over time upon sealing the sample. **(C)** The mean pO_2 vs time graph shows the decreasing trend of pO_2 due to oxygen consumption by MCF7 cells ($p<<0.001$, one way ANOVA).

Discussion

In this study, Nile Red doped HMDSO based nanoprobes were successfully formulated for fluorescence imaging and ^{1}H MRI based oximetry. A surfactant combination consisting of Solutol HS15 and soybean lecithin was used to emulsify HMDSO. Solutol HS-15 is a non-ionic emulsifier and drug solubilizer containing hydrophilic polyethylene glycol (PEG) and lipophilic 12-hydroxystearic acid. Soybean lecithin is primarily composed of L-α-phosphatidyl choline. Lecithin is frequently used in the preparation of nanoemulsions for drug delivery to the area of interest [37] while Solutol HS15 has been used as a solubilizer or co-surfactant in the preparation of various nanoemulsions [38]. Both surfactants are nonionic and ampiphilic which aids in encapsulating and transporting the hydrophobic HMDSO doped with the fluorophore into the interior of the cell.

Particles of radius less than 5 nm are rapidly cleared by the kidneys (renal clearance) while particles of radius larger than 100 nm are removed via phagocytosis [39]. Our nanoprobes showed distribution with mean droplet radius in the 70 nm range. Although the ideally we would prefer nanoprobes of radius < 50 nm for systemic delivery in vivo, it is difficult to precisely control the droplet sizes in nanoemulsions. The size range of the droplets depends on numerous parameters such as type of surfactants used, thermodynamic conditions and time and method of preparation [40] . Even using the extrusion method, we observe droplet sizes greater than the filter pore size due to the deformability of the emulsion. The observed HMDSO to water ratio of 0.69 exceeds the theoretically expected ratio of 0.54. This indicates that there is no loss of HMDSO during the emulsification process, though some water may have evaporated. The nanoprobes also maintained consistent particle size in water and 50% human plasma for 24 hours indicating that there will be little to no aggregation in body fluids when used *in vivo*. This could also prevent rapid clearance of the nanoprobes from the body. Particle sizes were seen to be smaller in plasma than in water, presumably due to the higher viscosity and lower surface tension of the continuous phase [41]. The surfactant combinations showed no cytotoxicity towards 3T3 cells up to a concentration of 1% (v/v). This is in accordance with published studies which show that Solutol HS15 has very low toxicity when used *in vivo*. [42] Similarly, lecithin is not expected to show toxicity in vivo as it is a component of biological membranes and is frequently used in nano/micro emulsion formulation and even in food preparation [43]. Our nanoprobes prepared using this surfactant combination, however, showed IC_{50} at a concentration of 0.4% (v/v). We can thus infer that incubating cells with nanoprobe concentrations greater than 0.4% (v/v) would not be feasible for cell tracking experiments. Live and fixed cell imaging experiments helped in the visualization of nanoprobes within the cytosol of MCF7 cells within 18 minutes of incubation. This indicates that our nanoprobes containing hydrophobic HMDSO successfully overcame the cell membrane barriers and could be transported into and localized within the cells.

Finally, the dual modality experiment was conducted to test the dual functionality of the nanoprobes. Fluorescence imaging showed ability to detect the nanoprobes at concentrations appropriate for in vivo use. Oximetry using the PISTOL technique on the same sample allowed non-invasive mapping of oxygen tension over time and allowed the estimation of oxygen consumption. The measured values of oxygen consumption are within the range measured *in vitro* by other groups [44-46] for cells under various physiological conditions. We incorporated 10%(v/v) matrigel for these studies. Our observed signal-to-noise ratios (SNR) for the corresponding MR images were 134 for the longest recovery time (TR) image (TR =55 s, 1 signal average [21]) and 9 for the shortest TR image (TR=0.1 s, 8 signal averages [21]). This indicates that 5-10 fold reduction of nanoemulsion in the matrigel would still have allowed us to perform oximetry, although sensitivity limits were not tested. For MRI, the in vitro sensitivity estimates would translate well to the in vivo case. The observed SNR for the corresponding fluorescence image was 14995. While the corresponding extrapolation of this observation to in vivo fluorescence studies is confounded by light scattering and absorption in vivo, the observed SNR indicates that 3 orders of magnitude reduction in concentration would still be detectable by fluorescence. Thus cell-labeling and implantation studies at concentrations well below the IC_{50} could be feasible for tracking by in vivo fluorescence imaging. Further improvement for in vivo application could include replacement of Nile Red dye with other hydrophobic dyes that fluoresce in the near-infrared region [9, 47].

In conclusion, we have successfully developed HMDSO-based dual modality and dual-functional nanoprobes that can be simultaneously used for fluorescence imaging and oximetry. These nanoprobes have the potential for theranostic applications by incorporation of poorly soluble drugs in the hydrophobic HMDSO core. Another potential application of these nanoprobes can be for tracking implanted cells while simultaneously monitoring cell health via ^{1}H

MR. While analogous ^{19}F based perfluorocarbon emulsions have been successfully used for cell tracking, a ^{1}H MR based approach has better potential for wider applicability.

Acknowledgments

The authors would like to thank Dr. Xiankai Sun for the use of the dynamic light scattering instrument and Abhijit Bugde for assistance with the live cell fluorescence microscopy. NIH-3T3 fibroblast cells were kindly provided by Prof. Liping Tang of University of Texas at Arlington. This work was supported by Norman Hackerman ARP grant #010019-0056-2007, NCI 1R21CA132096-01A1 and NCI U24 CA126608A.

Competing Interests

The authors have declared that no competing interest exists.

References

[1] Lum JJ, Bui T, Gruber M, Gordan JD, DeBerardinis RJ, Covello KL, et al. The transcription factor HIF-1alpha plays a critical role in the growth factor-dependent regulation of both aerobic and anaerobic glycolysis. Genes Dev. 2007;21:1037-49.

[2] Wachsberger P, Burd R, Dicker AP. Tumor Response to Ionizing Radiation Combined with Antiangiogenesis or Vascular Targeting Agents. Clinical Cancer Research. 2003;9:1957-71.

[3] Harrison L, Blackwell K. Hypoxia and anemia: factors in decreased sensitivity to radiation therapy and chemotherapy? Oncologist. 2004;9 Suppl 5:31-40.

[4] Cancedda R, Dozin B, Giannoni P, Quarto R. Tissue engineering and cell therapy of cartilage and bone. Matrix Biology. 2003;22:81-91.

[5] Volkmer E, Drosse I, Otto S, Stangelmayer A, Stengele M, Kallukalam BC, et al. Hypoxia in static and dynamic 3D culture systems for tissue engineering of bone. Tissue engineering Part A. 2008;14:1331-40.

[6] Potier E, Ferreira E, Meunier A, Sedel L, Logeart-Avramoglou D, Petite H. Prolonged hypoxia concomitant with serum deprivation induces massive human mesenchymal stem cell death. Tissue engineering. 2007;13:1325-31.

[7] Femandes TG, Diogo MM, Femandes-Platzgummer A, Lobato da Silva C, Cabral JMS. Effect of hypoxia on proliferation and neural commitment of embryonic stem cells at different stages of pluripotency. Bioengineering (ENBENG), 2011 ENBENG 2011 1st Portuguese Meeting. 2011:1-4.

[8] Bulte JWM, Kraitchman DL. Iron oxide MR contrast agents for molecular and cellular imaging. NMR in biomedicine. 2004;17:484-99.

[9] Bhirde A, Xie J, Swierczewska M, Chen X. Nanoparticles for cell labeling. Nanoscale. 2011;3:142-53.

[10] Bulte JW. In vivo MRI cell tracking: clinical studies. AJR American journal of roentgenology. 2009;193:314-25.

[11] Bulte JW, Kraitchman DL. Monitoring cell therapy using iron oxide MR contrast agents. Current pharmaceutical biotechnology. 2004;5:567-84.

[12] Temme S, Bonner F, Schrader J, Flogel U. 19F magnetic resonance imaging of endogenous macrophages in inflammation. Wiley interdisciplinary reviews Nanomedicine and nanobiotechnology. 2012;4:329-43.

[13] Boehm-Sturm P, Mengler L, Wecker S, Hoehn M, Kallur T. In vivo tracking of human neural stem cells with 19F magnetic resonance imaging. PloS one. 2011;6:e29040.

[14] Hitchens TK, Ye Q, Eytan DF, Janjic JM, Ahrens ET, Ho C. 19F MRI detection of acute allograft rejection with in vivo perfluorocarbon labeling of immune cells. Magnetic Resonance in Medicine. 2011;65:1144-53.

[15] Zhang H. Perfluoro-15-crown-5 ether-labeled dendritic cells. Molecular Imaging and Contrast Agent Database (MICAD). Bethesda (MD). 2004.

[16] Partlow KC, Chen J, Brant JA, Neubauer AM, Meyerrose TE, Creer MH, et al. 19F magnetic resonance imaging for stem/progenitor cell tracking with multiple unique perfluorocarbon nanobeacons. FASEB journal : official publication of the Federation of American Societies for Experimental Biology. 2007;21:1647-54.

[17] Mason RP, Zhao D, Pacheco-Torres J, Cui W, Kodibagkar VD, Gulaka PK, et al. Multimodality imaging of hypoxia in preclinical settings. Q J Nucl Med Mol Imaging. 2010;54:259-80.

[18] Zhao D, Jiang L, Mason RP. Measuring changes in tumor oxygenation. Methods in enzymology. 2004;386:378-418.

[19] Kodibagkar VD, Wang X, Pacheco-Torres J, Gulaka P, Mason RP. Proton imaging of siloxanes to map tissue oxygenation levels (PISTOL): a tool for quantitative tissue oximetry. NMR in biomedicine. 2008;21:899-907.

[20] Kodibagkar VD, Cui W, Merritt ME, Mason RP. Novel ^{1}H NMR approach to quantitative tissue oximetry using hexamethyldisiloxane. Magnetic Resonance in Medicine. 2006;55:743-8.

[21] Gulaka PK, Rastogi U, McKay MA, Wang X, Mason RP, Kodibagkar VD. Hexamethyldisiloxane-based nanoprobes for ^{1}H MRI oximetry. NMR in biomedicine. 2011;24:1226-34.

[22] Solans C, Izquierdo P, Nolla J, Azemar N, Garcia-Celma MJ. Nano-emulsions. Curr Opin Colloid In. 2005;10:102-10.

[23] Wang XY, Ju S, Li C, Peng XG, Chen AF, Mao H, et al. Non-invasive Imaging of Endothelial Progenitor Cells in Tumor Neovascularization Using a Novel Dual-modality Paramagnetic/Near-Infrared Fluorescence Probe. PloS one. 2012;7:e50575.

[24] Jarzyna PA, Deddens LH, Kann BH, Ramachandran S, Calcagno C, Chen W, et al. Tumor angiogenesis phenotyping by nanoparticle-facilitated magnetic resonance and near-infrared fluorescence molecular imaging. Neoplasia. 2012;14:964-73.

[25] Key J, Cooper C, Kim AY, Dhawan D, Knapp DW, Kim K, et al. In vivo NIRF and MR dual-modality imaging using glycol chitosan nanoparticles. Journal of controlled release. 2012;163:249-55.

[26] Bumb A, Regino CA, Egen JG, Bernardo M, Dobson PJ, Germain RN, et al. Trafficking of a dual-modality magnetic resonance and fluorescence imaging superparamagnetic iron oxide-based nanoprobe to lymph nodes. Molecular imaging and biology. 2011;13:1163-72.

[27] Kessinger CW, Khemtong C, Togao O, Takahashi M, Sumer BD, Gao J. In vivo angiogenesis imaging of solid tumors by alpha(v)beta(3)-targeted, dual-modality micellar nanoprobes. Exp Biol Med. 2010;235:957-65.

[28] Zhou J, Sun Y, Du X, Xiong L, Hu H, Li F. Dual-modality in vivo imaging using rare-earth nanocrystals with near-infrared to near-infrared (NIR-to-NIR) upconversion luminescence and magnetic resonance properties. Biomaterials. 2010;31:3287-95.

[29] Xu H, Regino CA, Koyama Y, Hama Y, Gunn AJ, Bernardo M, et al. Preparation and preliminary evaluation of a biotin-targeted, lectin-targeted dendrimer-based probe for dual-modality magnetic resonance and fluorescence imaging. Bioconjugate chemistry. 2007;18:1474-82.

[30] Uzgiris EE, Sood A, Bove K, Grimmond B, Lee D, Lomnes S. A multimodal contrast agent for preoperative MR Imaging and intraoperative tumor margin delineation. Technology in cancer research & treatment. 2006;5:301-9.

[31] Talanov VS, Regino CA, Kobayashi H, Bernardo M, Choyke PL, Brechbiel MW. Dendrimer-based nanoprobe for dual modality magnetic resonance and fluorescence imaging. Nano letters. 2006;6:1459-63.

[32] Lalande C, Miraux S, Derkaoui SM, Mornet S, Bareille R, Fricain JC, et al. Magnetic resonance imaging tracking of human adipose derived stromal cells within three-dimensional scaffolds for bone tissue engineering. European cells & materials. 2011;21:341-54.

[33] Kamaly N, Kalber T, Kenny G, Bell J, Jorgensen M, Miller A. A novel bimodal lipidic contrast agent for cellular labelling and tumour MRI. Organic & biomolecular chemistry. 2010;8:201-11.

[34] Montet-Abou K, Daire JL, Hyacinthe JN, Jorge-Costa M, Grosdemange K, Mach F, et al. In vivo labelling of resting monocytes in the reticuloendothelial system with fluorescent iron oxide nanoparticles prior to injury reveals that they are mobilized to infarcted myocardium. European heart journal. 2010;31:1410-20.

[35] Modo M, Mellodew K, Cash D, Fraser SE, Meade TJ, Price J, et al. Mapping transplanted stem cell migration after a stroke: a serial, in vivo magnetic resonance imaging study. NeuroImage. 2004;21:311-7.

[36] Wei L, Li G, Yan YD, Pradhan R, Kim JO, Quan Q. Lipid emulsion as a drug delivery system for breviscapine: formulation development and optimization. Archives of pharmacal research. 2012;35(6):1037-43.

[37] Hoeller S, Sperger A, Valenta C. Lecithin based nanoemulsions: A comparative study of the influence of non-ionic surfactants and the cationic phytosphingosine on physicochemical behaviour and skin permeation. International Journal of Pharmaceutics. 2009;370:181-6.

[38] Jain R, Patravale VB. Development and evaluation of nitrendipine nanoemulsion for intranasal delivery. J Biomed Nanotechnol. 2009;5:62-8.
[39] Bhowmik BB, Sa B, Mukherjee A. Preparation and in vitro characterization of slow release testosterone nanocapsules in alginates. Acta Pharm. 2006;56:417-29.
[40] Porras M, Solans C, González C, Martínez A, Guinart A, Gutiérrez JM. Studies of formation of W/O nano-emulsions. Colloids and Surfaces A: Physicochemical and Engineering Aspects. 2004;249:115-8.
[41] Mason TG, Wilking JN, Meleson K, Chang CB, Graves SM. Nanoemulsions: formation, structure, and physical properties. J Phys-Condens Mat. 2006;18:R635-R66.
[42] Coon JS, Knudson W, Clodfelter K, Lu B, Weinstein RS. Solutol HS 15, Nontoxic Polyoxyethylene Esters of 12-Hydroxystearic Acid, Reverses Multidrug Resistance. Cancer research. 1991;51:897-902.
[43] Paolino D, Ventura CA, Nisticò S, Puglisi G, Fresta M. Lecithin microemulsions for the topical administration of ketoprofen: percutaneous adsorption through human skin and in vivo human skin tolerability. International Journal of Pharmaceutics. 2002;244:21-31.
[44] Shen J, Khan N, Lewis LD, Armand R, Grinberg O, Demidenko E, et al. Oxygen consumption rates and oxygen concentration in molt-4 cells and their mtDNA depleted (rho0) mutants. Biophysical journal. 2003;84:1291-8.
[45] Streeter I, Cheema U. Oxygen consumption rate of cells in 3D culture: the use of experiment and simulation to measure kinetic parameters and optimise culture conditions. The Analyst. 2011;136:4013-9.
[46] Diepart C, Verrax J, Calderon PB, Feron O, Jordan BF, Gallez B. Comparison of methods for measuring oxygen consumption in tumor cells in vitro. Analytical biochemistry. 2010;396:250-6.
[47] He X, Gao J, Gambhir SS, Cheng Z. Near-infrared fluorescent nanoprobes for cancer molecular imaging: status and challenges. Trends in molecular medicine. 2010;16:574-83.